

to be published in Astronomy Letters, 2017, v. 43, n. 7, pp. 464–470

THE ORIGIN OF THE BIMODAL LUMINOSITY DISTRIBUTION OF ULTRALUMINOUS X-RAY PULSARS

S.A. Grebenev*

*Space Research Institute, Russian Academy of Sciences,
Profsoyuznaya ul. 84/32, Moscow, 117997 Russia*

Submitted on November 14, 2016

The mechanism that can be responsible for the bimodal luminosity distribution of super-Eddington X-ray pulsars in binary systems is pointed out. The transition from the high to low state of these objects is explained by accretion flow spherization due to the radiation pressure at certain (high) accretion rates. The transition between the states can be associated with a gradual change in the accretion rate. The complex behavior of the recently discovered ultraluminous X-ray pulsars M 82 X-2, NGC 5907 ULX-1, and NGC 7793 P13 is explained by the proposed mechanism. The proposed model also naturally explains the measured spinup of the neutron star in these pulsars, which is slower than the expected one by several times.

DOI: 10.1134/S1063773717050012

Keywords: ultraluminous X-ray sources, supercritical accretion, X-ray pulsars, neutron stars, bimodality.

* E-mail <sergei@hea.iki.rssi.ru>

INTRODUCTION

The discovery (Bachetti et al. 2014) of X-ray pulsations with a mean period $P_s \simeq 1.37$ s from the ultraluminous X-ray (ULX) source M 82 X-2 (=NuSTAR J095551+6940.8) and its sinusoidal modulation with a period $P_b \simeq 2.5$ days (the orbital period of the binary system) changed drastically our views of the nature of ULX sources. Previously, it had been assumed that a high observed isotropic X-ray luminosity of such sources $L_{\text{iso}} \gtrsim 10^{40}$ erg s⁻¹ could be reached only during accretion onto a black hole with a moderately large, $\sim 10^3 M_\odot$, or at least stellar, $\sim 10 M_\odot$, mass (provided the formation of a relativistic jet and associated strong radiation anisotropy). It has now become clear that such a luminosity can also take place during accretion onto a neutron star possessing a strong magnetic field with a mass of only $M_* \sim 1.4 M_\odot$. Such binary systems must be widespread and can even dominate in the population of ULX sources (Shao and Li 2015). The discoveries of the ultraluminous X-ray pulsars NGC 7793 P13 and NGC 5907 ULX-1 by the XMM-Newton satellite (Israel et al. 2017a, 2017b) shortly afterward confirm this point of view and give hope for the detection of other objects of this type. Note that NGC 5907 ULX-1 has a record peak luminosity even for ULX sources, in particular, it exceeds the maximum detected luminosity of M 82 X-2 by several times (see the table).

The discovery of ULX pulsars has thrown down a serious challenge to theorists. For example, it is still unclear, though is widely discussed, how such a high luminosity is reached, which exceeds the Eddington one for spherically symmetric accretion onto a neutron star by hundreds of times:

$$L_{\text{ed}} = \frac{4\pi G M_* m_p c}{\sigma_{\text{es}}} \simeq 1.9 \times 10^{38} \left(\frac{\sigma_{\text{T}}}{\sigma_{\text{es}}} \right) \left(\frac{M_*}{1.4 M_\odot} \right) \text{ erg s}^{-1}. \quad (1)$$

Here, σ_{es} is the electron scattering cross section, σ_{T} is the Thomson cross section, G is the gravitational constant, m_p is the proton mass, and c is the speed of light. Of course, the accretion onto a neutron star with a strong magnetic field is far from spherically symmetric one. As early as 1976, having considered a realistic accretion flow geometry at a supercritical accretion rate, Basko and Sunyaev (1976) showed that the isotropic luminosity of a pulsar could exceed L_{ed} by more than an order of magnitude (see below). Nevertheless, it is still insufficient to explain the observations of ULX pulsars.

Many of the authors (e.g., Lyutikov 2014; Tong 2015; Eksi et al. 2015; Tsygankov et al. 2016a; Israel et al. 2017a, 2017b) are inclined to the assumption about an extreme

Table. Parameters of the ULX pulsars discovered to date, their corotation, magnetospheric, and spherization radii

Source	General								In high state		In low state	
	P_b^a days	P_s s	\dot{P}_{-10} s s $^{-1}$	γ_s	μ_3	R_c^e km	\dot{M}_{20}^f g s $^{-1}$	R_s^e km	L_{39}^g erg s $^{-1}$	R_m^e km	L_{39}^g erg s $^{-1}$	R_{ms}^h km
M 82 X-2	2.5	1.37	-2.0	4	3	2080	0.59	860	37	900	0.28	890
NGC 5907 ULX-1	5.3	1.13	-8.1	6	12	1830	1.06	1550	100	1670	0.3	1640
NGC 7793 P13		0.42	-0.4	2	1.4	950	0.41	610	13	640	0.3	630

^a The orbital period P_b .

^b The pulsar period P_s and mean period derivative $\dot{P}_s = 10^{-10} \dot{P}_{-10}$.

^c The presumed factor of the emission anisotropy.

^d The presumed magnetic momentum of the neutron star $\mu = 3 \times 10^{30} \mu_3 \text{ G cm}^3$.

^e The corotation, R_c , spherization, R_s , and magnetospheric, R_m , radii.

^f The presumed accretion rate $\dot{M}_0 = 10^{20} \dot{M}_{20}$ corresponding to the luminosity L_{39} in the high state (according to $L_{\text{iso}}^{\text{obs}} = \gamma GM_* \dot{M}_0 / R_*$).

^g The observed isotropic X-ray luminosity $L_{\text{iso}}^{\text{obs}} = 10^{39} L_{39}$ in the energy range 0.3–10 keV.

^h The magnetospheric radius in the low state according to Eq. (11).

magnetic field strength of the neutron star in ULX systems ($B_* \gtrsim 10^{14} \text{ G}$), which reduces the electron scattering cross section σ_{es} and, thus, raises the Eddington limit. Others (e.g., Kluzniak and Lasota 2015) think that a high luminosity is reached precisely because of the reduced (to $B_* \sim 10^9 \text{ G}$) magnetic field strength (compared to its values $B_* \sim 10^{12} - 10^{13} \text{ G}$ typical for X-ray pulsars). Because of the weak magnetic field, the accretion disk almost reaches the neutron star surface and radiates in the same way as during super-Eddington accretion onto a black hole. In both cases, the limiting observed luminosity of ULX pulsars, $L_{\text{iso}} \sim 10^{41} \text{ erg s}^{-1}$, still cannot be explained and one has to appeal to a strong anisotropy of their radiation (dall’Osso et al. 2015; Chen 2017).

The nature of the bimodal luminosity distribution of ULX pulsars pointed out by Tsygankov et al. (2016a) and Israel et al. (2017a, 2017b) also remains a puzzle. In addition to the state with a very high X-ray luminosity (hereafter the high state), periods during which the luminosity dropped to $\lesssim 3 \times 10^{38} \text{ erg s}^{-1}$ (hereafter the low state) have been detected for all three sources (see the table). Tsygankov et al. (2016a) and Israel et al. (2017) assumed the bimodality of the luminosity distribution to be associated with the action of centrifugal forces, which inhibit accretion and are capable of expelling an excess of accreting matter from the system (the propeller effect; Illarionov and Sunyaev 1975; see also Corbet 1996). This effect begins to manifest itself as soon as the magnetospheric radius of the neutron star R_m during the evolution of the system (for example, a temporary decrease in the accretion rate) exceeds the corotation radius R_c (otherwise the surface rotation velocity of the mag-

netosphere will exceed the Keplerian velocity). In this case, the accretion onto the neutron star ceases, and only the radiation from the outer disk region $R > R_m$ is observed. In order for the propeller effect to operate in the systems being discussed, it is necessary that the neutron stars in them possess a very strong magnetic field $B_* \sim 10^{14} - 10^{15}$ G similar to the field of magnetars (Tsygankov et al. 2016a).

Although the very existence of the propeller effect is beyond doubt and has come into wide use by astrophysicists, i.e., it is used to explain the observed luminosity jumps in millisecond (LMXBs, Campana et al. 2008, 2014) and ordinary (HMXBs, Corbet et al. 1996; Campana et al. 2002; Tsygankov et al. 2016b; Postnov et al. 2017) X-ray pulsars, the existence of “equilibrium” pulsar periods (van den Heuvel 1984; Corbet 1986), the outbursts of fast X-ray transients (Grebenev and Sunyaev 2007; Grebenev 2009), and many other observed phenomena, the action of this mechanism as a cause of the bimodal luminosity distribution of ULX pulsars raises doubts. This is not only due to the very strong neutron star magnetic field, $B_* \gtrsim 10^{14}$ G, required for this purpose, but also due to the observed range of the luminosity drop, which is smaller by several times than the expected one $\sim R_c/R_* \simeq 140 m_*^{1/3} p_*^{2/3} R_{12}^{-1}$ (Corbet 1996; Tsygankov et al. 2016a; here, p_* is the spin period of the neutron star P_s in seconds, while m_* and R_{12} are its mass M_* and radius R_* normalized to their standard values of $1.4 M_\odot$ 12 km), and, most importantly, the very close coincidence of the luminosity of the sources in their low state with the Eddington one L_{ed} . In this paper we will show that there exists a different explanation for the abrupt change of the luminosity in these sources associated with the transitions between two different regimes of supercritical accretion onto a neutron star with a strong magnetic field. The transitions are caused by accretion flow spherization in the disk due to the radiation pressure when a certain accretion rate dependent on the magnetic field strength of the neutron star is exceeded.

THE REGIMES OF SUPERCRITICAL ACCRETION

The properties of the accretion flow onto a neutron star and the interaction of this flow with its magnetic field are defined by four characteristic radii:

The *magnetospheric radius*

$$R_m \simeq \xi \left(\frac{\mu_*^2}{\sqrt{2GM_*\dot{M}}} \right)^{2/7} \simeq 8.2 \times 10^7 \xi \mu_3^{4/7} m_*^{-1/7} \dot{m}_{20}^{-2/7} \text{ cm}, \quad (2)$$

at which the pressure of the matter inflowing through the accretion disk is equal to the

pressure of the neutron star magnetic field (Davidson and Ostriker 1973; Illarionov and Sunyaev 1975);

the *spherization radius* of the accretion flow

$$R_s = \frac{3}{8\pi} \frac{\dot{M}_0}{m_p} \frac{\sigma_T}{c} = \frac{3}{2} \frac{GM_* \dot{M}_0}{L_{\text{ed}}} \simeq 1.5 \times 10^8 \dot{m}_{20} \text{ cm}, \quad (3)$$

at which the accretion disk under radiation pressure swells so that its half-thickness is equal to the radius R (Shakura and Sunyaev 1973)¹;

the *corotation radius*

$$R_c = \left(\frac{GM_* P_s^2}{4\pi^2} \right)^{1/3} = 1.7 \times 10^8 m_*^{1/3} p_*^{2/3} \text{ cm}, \quad (4)$$

at which the surface rotation velocity of the magnetosphere $(2\pi/P_s)R_c$ is equal to the Keplerian velocity $(GM_*/R_c)^{1/2}$ (Illarionov and Sunyaev 1975);

and, of course, the *intrinsic radius* of the neutron star R_* .

Here, $\xi \simeq 0.5$ is the correction that takes into account the deviation of the magnetospheric radius in the case of disk accretion from the Alfvén radius computed for spherically symmetric accretion (Ghosh and Lamb 1978), \dot{m}_{20} is the accretion rate \dot{M}_0 in units of 10^{20} g s^{-1} ($= 1.6 \times 10^{-6} M_\odot \text{ yr}^{-1}$), $\mu_* = 0.5 B_* R_*^3$ is the dipole magnetic moment of the neutron star, and B_* is the magnetic field strength at its poles. The magnetic moment μ_* expressed in units of $3 \times 10^{30} \text{ G cm}^3$ will be denoted by μ_3 . Note that by \dot{M} in Eq. (2) we mean the accretion rate near the magnetospheric boundary. During super-Eddington accretion in the inner disk regions \dot{M} can decrease compared to the external value \dot{M}_0 due to the outflow of matter.

In Fig. 1 the radii R_m , R_s , and R_c are plotted against the accretion rate for three magnetic moments of the neutron star, $\mu_3 = 0.1, 1$, and 10 . These values correspond to magnetic field strengths at the stellar poles $B_* \simeq 3.5 \times 10^{11}, 3.5 \times 10^{12}, 3.5 \times 10^{13} \text{ G}$, respectively. The pulsation period was assumed to be 1.37 s , the same as that for the ULX pulsar M82 X-2. The estimates of the radii R_m , R_s , R_c for this and the two other ULX pulsars known to date are given in the table. As will be shown below, once R_s has reached R_m , the magnetospheric radius R_m ceases to depend on \dot{M}_0 . Therefore, the dependence (2) in this region is indicated in Fig. 1 by the dotted line.

¹The disk luminosity in the region $R > R_s$ turns out then to be equal to the Eddington luminosity $L_d = (3/2)GM_*\dot{M}_0/R_s = L_{\text{ed}}$ (Lipunova 1999).

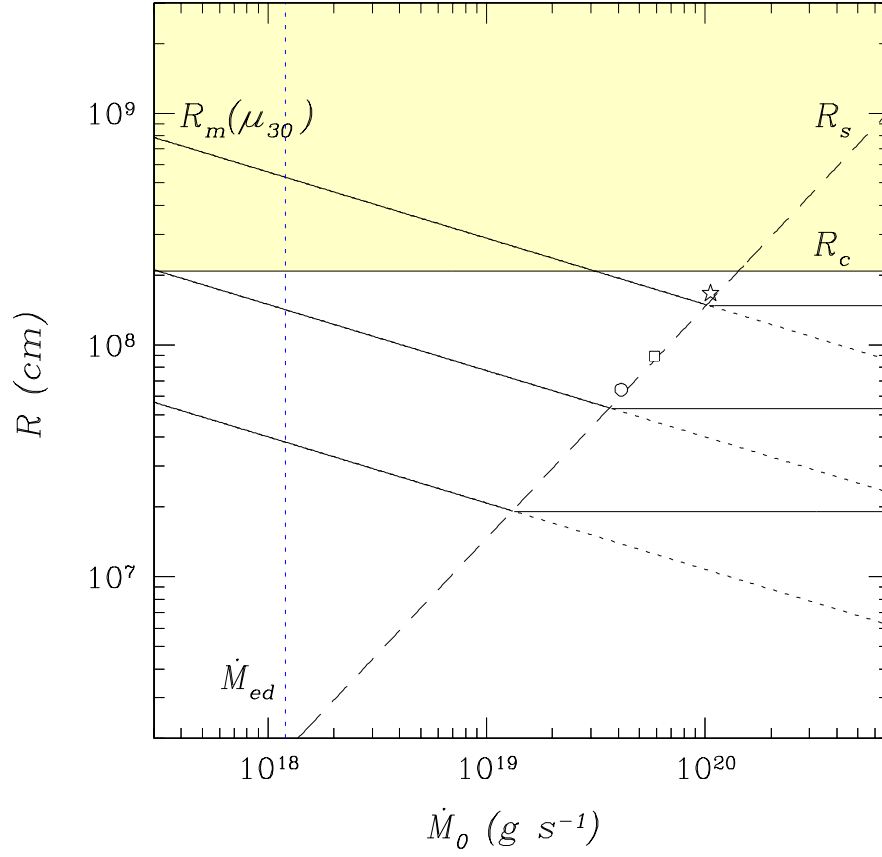


Fig. 1: Spherization radius of the accretion flow R_s (dashed line), corotation radius R_c (the lower boundary of the shaded region), and magnetospheric radius of the neutron star R_m (solid lines) versus accretion rate for an ultraluminous X-ray pulsar with the same period as that for M82 X-2. Different magnetic moments of the star are considered, $\mu_3 = 0.1, 1$, and 10 (the solid lines from the bottom upward). The shaded region corresponds to the radius R_m at which the propeller regime is realized. The vertical dotted line marks the Eddington accretion rate. Asterisk, square and circle show values of R_m and \dot{M}_0 adopted in the paper for the maximum high state of the ULX pulsars NGC 5907 ULX-1, M82 X-2, and NGC 7793 P13, respectively.

Figure 1 suggests that the dependence of the magnetospheric radius of the neutron star R_m on \dot{M}_0 has two singular points. This radius is equal to the corotation radius R_c and the spherization radius R_s at the first and second points, respectively. The first event occurs at an accretion rate

$$\dot{M}_{mc} \simeq 7.2 \times 10^{17} \mu_3^2 m_*^{-5/3} p_*^{-7/3} \text{ g s}^{-1}, \quad (5)$$

and the second one occurs at an accretion rate (Lipunov 1982)

$$\dot{M}_{ms} \simeq 3.7 \times 10^{19} \mu_3^{4/9} m_*^{-1/9} \text{ g s}^{-1}. \quad (6)$$

At $\dot{M}_0 \leq \dot{M}_{mc}$ no efficient accretion is possible because of the propeller effect — the infalling matter is ejected from the system. At $\dot{M}_0 \geq \dot{M}_{mc}$ and up to $\dot{M}_0 \simeq \dot{M}_{ms}$ nothing inhibits it;

the regime of direct accretion observed in ordinary X-ray pulsars with the modifications for $\dot{M}_0 \gtrsim \dot{M}_{\text{ed}} = L_{\text{ed}} R_*/(GM_*) \simeq 1.2 \times 10^{18} \text{ g s}^{-1}$, described by Basko and Sunyaev (1976), is realized. Note that in this regime the spherization radius $R_s < R_m$. Let us consider the case of direct supercritical accretion in more detail.

The High State (an Accretion Rate $\dot{M}_{mc} \leq \dot{M}_0 \leq \dot{M}_{ms}$)

In this case, just as in the case of ordinary X-ray pulsars, upon reaching the boundary of the magnetosphere, the accretion disk matter is frozen into its upper layer and is transferred by two streams to high-latitude regions, where it flows down along the so-called accretion columns into the vicinity of the neutron star magnetic poles. Basko and Sunyaev (1976) (see also Lyubarskii and Sunyaev 1988; Mushtukov et al. 2015) showed that at $\dot{M}_0 \gtrsim \dot{M}_{\text{ed}}$ the radiation flux escaping through the walls of the accretion columns in X-ray pulsars exceeds the radial (Eddington) flux by a factor of $\sim H/d \simeq 240 R_{12} (H/R_*)$; accordingly, their total luminosity

$$L_{\text{iso}} = 4Hl \left(\frac{H}{d} \right) \left(\frac{L_{\text{ed}}}{4\pi R_*^2} \right) = \frac{l}{\pi d} \left(\frac{H}{R_*} \right)^2 L_{\text{ed}}.$$

can exceed L_{ed} . Here, H is the height of the accretion columns², $l \simeq 2.5 \times 10^5 \text{ cm}$ is the width of their base, $d \simeq 5 \times 10^3 \text{ cm}$ is the thickness of the walls. Since typically $H \lesssim R_*$, the actual increase in luminosity is limited by

$$L_{\text{iso}}^{\text{max}} \lesssim 3 \times 10^{39} \left(\frac{l/d}{50} \right) \left(\frac{\sigma_{\text{T}}}{\sigma_{\text{es}}} \right) \left(\frac{M_*}{1.4 M_{\odot}} \right) \text{ erg s}^{-1}. \quad (7)$$

The luminosity of the accretion disk $L_{\text{d}} \lesssim L_{\text{ed}}$ should be added to the luminosity of the accretion columns L_{iso} , but still, to achieve agreement with the observations of ULX pulsars, it is necessary either to assume an appreciable radiation anisotropy or to take into account the decrease in the scattering cross section due to a strong magnetic field (Basko and Sunyaev 1975, 1976). Indeed, in the presence of a magnetic field at energies $E < E_B = 11.6 (B_*/10^{12} \text{ G}) \text{ keV}$ the electron scattering cross section σ_{es} decreases compared to the Thomson one as $\sigma_{\text{X}} \simeq \sigma_{\text{T}} (E/E_B)^2$ for the extraordinary wave and as $\sigma_{\text{O}} \simeq \sigma_{\text{T}} [\sin^2 \theta + (E/E_B)^2]$ for the ordinary one; here, θ is the angle between the direction of wave propagation and the magnetic field lines. Since the emergent radiation is multiply scattered in the accretion column walls, with the ordinary and extraordinary waves being transformed into one another, the effective scattering cross section in the standard X-ray band ($E \lesssim 10 \text{ keV}$) can be appreciably

²To be more precise, the height of the radiation-dominated shock in which the matter sinking in the column walls is heated to high temperatures above the neutron star surface.

smaller than σ_T (Paczynski 1992). Introducing an anisotropy factor $\gamma > 1$, suggesting that the radiation intensity toward us is greater than the mean intensity by a factor of γ , from inequality (7) we finally obtain

$$L_{\text{aniso}}^{\text{max}} \lesssim 3 \times 10^{40} \left(\frac{\gamma \sigma_T / \sigma_{\text{es}}}{10} \right) m_* \text{ erg s}^{-1}. \quad (8)$$

The parameter $\epsilon = \gamma (\sigma_T / \sigma_{\text{es}})$, which we set equal to 10, characterizes the joint uncertainty in the anisotropy of the emergent radiation and the decrease in the scattering cross section. The pulse profile for ULX pulsars is fairly smooth, nearly sinusoidal (Bachetti et al. 2014; Israel et al. 2017a, 2017b). Given that it is shaped by the radiation emerging from the walls of the accretion columns, it is hard to expect a very strong anisotropy of this radiation. Below we assume that $\gamma = 2 - 4$.

If the accretion occurred with the maximum possible efficiency, then one would expect the observed luminosity to be

$$L_{\text{iso}}^{\text{obs}} = \gamma G M_* \dot{M}_0 / R_* \simeq 1.6 \times 10^{40} \gamma R_{12}^{-1} m_* \dot{m}_{20} \text{ erg s}^{-1}. \quad (9)$$

Comparing this expression with inequality (8), we see that the energy being released during accretion can be efficiently reprocessed into radiation only as long as $\dot{m}_{20} \leq 0.2 R_{12} (\sigma_T / \sigma_{\text{es}})$. As the accretion rate increases further, no rise in luminosity occurs, the excess of energy being released is carried away to the neutron star surface (Basko and Sunyaev 1976). Note that the adopted values of ϵ and γ allow the observed maximum luminosities of the ULX pulsars M 82 X-2 and NGC 7793 P13 to be explained (see the table). In the case of NGC 5907 ULX-1, however, $\epsilon = \gamma (\sigma_T / \sigma_{\text{es}})$ and especially γ should be additionally increased by a factor of 2–3. A much stronger magnetic field apparently operates in this source, which leads to a more noticeable decrease in the scattering cross section σ_{es} , a more significant increase in the Eddington limit, and a more strong anisotropy of the radiation.

The Low State (a High Accretion Rate $\dot{M}_0 \geq \dot{M}_{ms}$)

The spherization radius is equal to R_m at an accretion rate $\dot{M}_0 \simeq \dot{M}_{ms}$ and begins to exceed it as \dot{M}_0 increases further. In this case: (1) the accretion disk swells near R_s , (2) an efficient outflow of excess matter and angular momentum with a nearly parabolic velocity is formed above the disk at $R < R_s$, and (3) the accretion in the region $R_m < R < R_s$ occurs in a regime close to the spherically symmetric one with a rate decreasing as

$$\dot{M}(R < R_s) = \dot{M}_0 R / R_s \quad (10)$$

(Shakura and Sunyaev 1973; Lipunova 1999). The total luminosity of the source in this case does not exceed $\simeq 2 L_{\text{ed}}$. Half of it, $\simeq L_{\text{ed}}$, is emitted by the outer $R > R_s$ disk regions, and the other half is emitted by the inner envelope formed by the outflowing matter. Irrespective of precisely where and how the energy release occurs here, due to the quasi-sphericity of this envelope, the luminosity of the radiation leaving it cannot exceed $\simeq L_{\text{ed}}$, the remaining energy being released is spent on the acceleration of the outflowing matter³. In this sense, the observed picture has much in common with the photospheric expansion of the neutron star atmosphere during super-Eddington X-ray bursts (see, e.g., Lewin et al. 1993). Just as for bursts, depending on the accretion rate, the density of the outflowing matter and the size of its photosphere (inner envelope) and, accordingly, the effective temperature of the emergent radiation change.

Although, on the whole, the X-ray observations of ULX pulsars in their low state are consistent with $\simeq 2 L_{\text{ed}}$, at high accretion rates an increasingly large fraction of the radiation must fall into the ultraviolet and optical spectral ranges. Therefore, the X-ray luminosity in the low state for some of the sources can be appreciably below the Eddington level. This may be true for NGC 5907 ULX-1 (Israel et al. 2017a).

Because of the decrease in the accretion rate at $R < R_s$, the flux of matter reaching the boundary of the neutron star magnetosphere turns out to be equal only to $\dot{M}_0 R_m / R_s$. Accordingly, the magnetospheric radius R_m does not decrease with increasing \dot{M}_0 after reaching the critical accretion rate \dot{M}_{ms} (as $\dot{M}_0^{-2/7}$, see Eq. 2), but remains equal to its value at $\dot{M}_0 = \dot{M}_{ms}$,

$$R_m^{\text{low}} \simeq 5.4 \times 10^7 \mu_3^{4/9} m_*^{-1/9} \text{ cm.} \quad (11)$$

In Fig. 1 this part of the dependence of R_m on \dot{M}_0 is indicated by the solid horizontal line, while the dependence (2) is indicated by the dashed line.

The shaded region in Fig. 1 indicates the forbidden values of the magnetospheric radius that exceed the corotation radius, $R_m > R_c$. At such R_m a rapidly rotating neutron star-magnetosphere would produce a centrifugal barrier for the accreting matter, inhibiting its penetration inward — the propeller regime would be switched on. Previously, it has already

³Note that even formally the above solution (10) for the decrease in the accretion rate at $R < R_s$ was obtained by assuming that the *entire* energy being released at $R < R_s$ is spent on the radiation acceleration of the outflowing matter (Lipunova 1999). Therefore, the frequently encountered assertion that the inner region gives a logarithmic $\sim L_{\text{ed}} \ln(\dot{M}_0/\dot{M}_{\text{ed}})$ increase of the luminosity of the outer disk is incorrect.

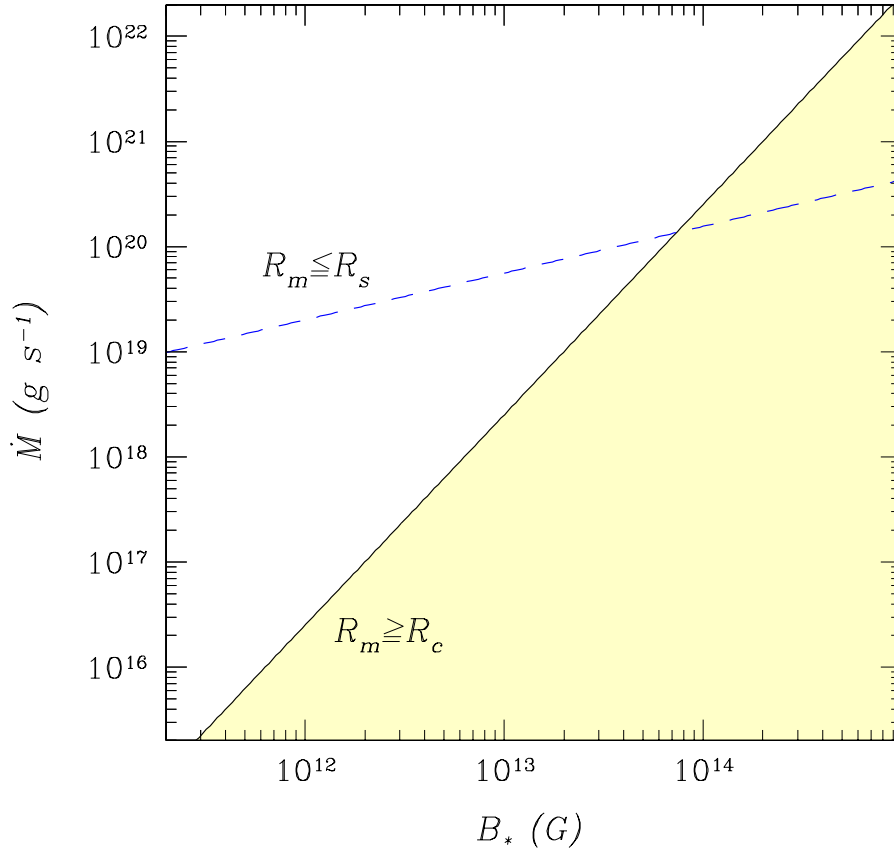


Fig. 2: The accretion rate \dot{M}_{mc} at which the magnetospheric radius R_m is equal to the corotation radius R_c (solid line) and the accretion rate \dot{M}_{ms} at which R_m is equal to the spherization radius R_s (dashed line) as functions of the neutron star magnetic field strength B_* . At $R_m > R_c$ (shaded) the direct accretion stops due to the propeller effect. At $R_m < R_s$ (above the dashed curve) the luminosity of the source is restricted by the Eddington limit, $L \lesssim 2L_{\text{ed}}$.

been mentioned that for this reason, no efficient accretion is possible at $\dot{M}_0 < \dot{M}_{mc}$. It can be seen from Fig. 1 that in the case of a strong magnetic field B_* , the situation when no direct accretion onto the neutron star is possible at any \dot{M}_0 is realistic. Figure 2 shows that this is actually the case. The solid line in this figure indicates the accretion rate \dot{M}_{mc} at which the magnetospheric radius R_m is equal to the corotation radius R_c (Eq. 5) as a function of the magnetic field strength B_* . In the shaded region to the right of this line $R_m \geq R_c$; therefore, no accretion is possible here due to the propeller effect. The dashed line in this figure indicates the accretion rate \dot{M}_{ms} at which the magnetospheric radius R_m is equal to the radius R_s (Eq. 6) as a function of B_* . Above this curve $R_m < R_s$. As has already been said, accretion flow spherization, a strong outflow of matter under radiation pressure, and a drop in luminosity to $\simeq 2L_{\text{ed}}$ begin here. Direct (efficient) accretion is possible only in the

$\dot{M}_0 - B_*$ region lying between these lines, to the left of their intersection. The limiting field at which direct accretion is still possible corresponds to the point of their intersection:

$$B_*^{\max} \simeq 4.4 \times 10^{13} R_{12}^{-3} m_* p_*^{3/2} \text{ G}. \quad (12)$$

However, it should be noted that at high accretion rates, when $R_m < R_s$, being in the shaded region in comparison with being outside it makes very little difference observationally — as before, we will see a source with a nearly Eddington total luminosity. This luminosity will be emitted by the accretion disk at large, $R > R_s$, distances from the neutron star and the outflowing envelope in the region $R_m^{\text{low}} < R < R_s$. Obviously, the accreting matter does not fall below the radius R_m^{low} , so that it is impossible to record any radiation pulsations in this regime of accretion. Given what has been said above about the softness of the radiation spectrum for such a source, it will most likely be impossible to determine whether the two-fold drop in its luminosity is associated with the excess of R_m above R_c or an excessively narrow and hard range of its observations.

THE NEUTRON STAR SPINUP RATE

Although the measured long-term spinup rate of the neutron star in the three discovered ULX pulsars, $\dot{\nu} = -\dot{P}_s P_s^{-2} \sim (1 - 6) \times 10^{-10} \text{ Hz s}^{-1}$, exceeds the spinup rate of the neutron star in ordinary X-ray pulsars by an order of magnitude or more (see the table), it turns out to be several times lower than the spinup rate expected for these sources, given the observed essentially super-Eddington accretion rate,

$$\dot{\nu} = (GM_* R_m)^{1/2} \frac{\dot{M}_0}{2\pi I} \simeq 1.4 \times 10^{-9} \dot{m}_{20}^{6/7} m_*^{3/7} \mu_3^{2/7} I_{45}^{-1} \text{ Hz s}^{-1}. \quad (13)$$

Here, I_{45} is the moment of inertia I_* of the neutron star (normalized to its standard value of 10^{45} g cm^2). Such a slow spinup is naturally explained in the scenario of supercritical accretion onto these pulsars proposed above. Indeed, the estimate (13) refers only to the high luminosity state of these sources. During their low state the actual accretion rate near the magnetosphere decreases considerably to $\dot{M}_0 R_m^{\text{low}}/R_s \simeq \dot{M}_{ms}$; the spinup rate of the neutron star drops accordingly. Moreover, it should be noted that in this state there is not disk accretion, which is capable of efficiently transferring the angular momentum of Keplerian motion to the neutron star, but almost quasi-spherical accretion of matter that lost much of its angular momentum. The angular momentum is transferred only in the narrow circular region which width is much smaller than the real width of the accretion disk. The foregoing

implies that an efficient spinup of the neutron star in the ULX pulsars occurs only during a certain fraction of the entire time of their active existence, while in the remaining time they barely spin up. For this reason, the mean spinup determined from long time intervals turns out to be appreciably smaller than their maximum spinup during the episodes of direct super-Eddington accretion.

CONCLUSIONS

We gave an explanation for the bimodality of the X-ray luminosity distribution of ULX pulsars. The transition from the high to low state of these sources was explained by accretion flow spherization when a certain accretion rate is exceeded. In this case, the luminosity of the source drops to a nearly Eddington level of $(1 - 2)L_{\text{ed}}$. The observed X-ray luminosity can be even lower, given the softness of the radiation spectrum forming in the envelope of matter outflowing from the accretion disk due to the radiation pressure. Apart from the rate of change of the accretion rate, the transition rate between the states is determined by the time it takes for the neutron star magnetosphere to be rearranged, the speed of the mass transfer through the disk, and the outflow velocity of the excess of matter.

The accretion-driven spinup rate of the neutron star in the low state decreases considerably compared to the spinup rate in the high state. This allows the mean, insufficiently high measured spinup rate of the ULX pulsars, lower than the expected one by several times at given accretion rates, to be explained.

ACKNOWLEDGMENTS

This work was financially supported by the Program of the President of the Russian Federation for support of leading scientific Schools (grant NSh-10222.2016.2) and the “Transitional and Explosive Processes in Astrophysics” Subprogram of the Basic Research Program P-7 of the Presidium of the Russian Academy of Sciences.

REFERENCES

1. M. Bachetti, F. A. Harrison, D. J. Walton, B. W. Grefenstette, D. Chakrabarty, F. Fürst, D. Barret, A. Beloborodov, et al., *Nature* **514**, 202 (2014).
2. M. M. Basko and R. A. Sunyaev, *Astron. Astrophys.* **42**, 311 (1975).
3. M. M. Basko and R. A. Sunyaev, *Mon. Not. Roy. Astron. Soc.* **175**, 395 (1976).
4. S. Campana, F. Brivio, N. Degenaar, S. Mereghetti, R. Wijnands, P. D’Avanzo, G.L. Israel, and L. Stella, *Mon. Not. Roy. Astron. Soc.* **441**, 1984 (2014).
5. S. Campana, L. Stella, G.L. Israel, A. Moretti, A.N. Parmar, and M. Orlandini, *Astrophys. J.* **580**, 389 (2002).
6. S. Campana, L. Stella, and J.A. Kennea, *Astrophys. J.* **684**, L99 (2008).
7. W.-C. Chen, *Mon. Not. Roy. Astron. Soc.* **465**, L6 (2017).
8. R. H. D. Corbet, *Mon. Not. Roy. Astron. Soc.* **220**, 1047 (1986).
9. R. H. D. Corbet, *Astrophys. J.* **457**, L31 (1996).
10. K. Davidson and J. P. Ostriker, *Astrophys. J.* **179**, 585 (1973).
11. K. Y. Eksi, I. C. Andac, S. Cikintoglu, A. A. Gencali, C. Güngör, and F. Öztekin, *Mon. Not. Roy. Astron. Soc.* **448**, L40 (2015).
12. P. Ghosh and F. K. Lamb, *Astrophys. J.* **223**, L83 (1978).
13. S. A. Grebenev, *Proceedings of Science*, **96**, 60 (Proc. of the Conference “The Extreme Sky: Sampling the Universe above 10 keV”, Otranto, Italy, October 13–17, 2009).
14. S. A. Grebenev and R. A. Sunyaev, *Astron. Lett.* **33**, 149 (2007).
15. E. P. J. van den Heuvel, *J. Astrophys. Astron.* **5**, 209 (1984).
16. A. F. Illarionov and R. A. Sunyaev, *Astron. Astrophys.* **39**, 185 (1975).
17. G. L. Israel, A. Belfiore, L. Stella, P. Esposito, P. Casella, A. De Luca, M. Marelli, A. Papitto, et al., *Science* **355**, 817; arXiv:1609.07375v1 (2017a).
18. G. L. Israel, A. Papitto, P. Esposito, L. Stella, L. Zampieri, A. Belfiore, G.A. Rodriguez Castillo, A. De Luca, et al., *Mon. Not. Roy. Astron. Soc.* **466**, L48; arXiv:1609.06538v1 (2017b).
19. W. Kluzniak and J.-P. Lasota, *Mon. Not. Roy. Astron. Soc.* **448**, L43 (2015).

20. W. H. G. Lewin, J. van Paradijs, and R. E. Taam, *Space Sci. Rev.* **62**, 223 (1993).
21. V. M. Lipunov, *Sov. Astron.* **26**, 54 (1982).
22. G. V. Lipunova, *Astron. Lett.* **25**, 508 (1999).
23. Yu. E. Lyubarskii and R. A. Sunayev, *Sov. Astron. Lett.* **14**, 390 (1988).
24. M. Lyutikov, *arXiv:1410.8745* (2014).
25. A. A. Mushtukov, V. F. Suleimanov, S. S. Tsygankov, and J. Poutanen, *Mon. Not. Roy. Astron. Soc.* **454**, 2539 (2015).
26. S. dall’Osso, R. Perna, and L. Stella, *Mon. Not. Roy. Astron. Soc.* **449**, 2144 (2015).
27. B. Paczynski, *Acta Astronomica* **42**, 145 (1992).
28. K. Postnov, L. Oskinova, and J.M. Torrejón, *Mon. Not. Roy. Astron. Soc.* **465**, L119 (2017).
29. N. I. Shakura and R. A. Sunyaev, *Astron. Astrophys.* **24**, 337 (1973).
30. Y. Shao and X.-D. Li, *Astrophys. J.* **802**, 131 (2015).
31. H. Tong, *Res. Astron. Astrophys.* **15**, 517 (2015).
32. S. S. Tsygankov, A. A. Mushtukov, V. F. Suleimanov, and J. Poutanen, *Mon. Not. Roy. Astron. Soc.* **457**, 1101 (2016a).
33. S. S. Tsygankov, A. A. Lutovinov, V. Doroshenko, A. A. Mushtukov, V. Suleimanov, and J. Poutanen, *Astron. Astrophys.* **593**, A16 (2016b).

Translated by V. Astakhov